Assessment of Gap and Charging Voltage Influence on Mechanical Behaviour of Joints Obtained by Magnetic Pulse Welding*

R. Raoelison[1], M. Rachik[1], N. Buiron[1], D. Haye[2], M. Morel[2], B. Dos Sanstos[2], D. Jouaffre[2], G. Frantz[3]

[1] Laboratoire Roberval, Université de Technologie de Compiègne, France,
[2] PFT INNOVALTECH, Saint-Quentin, France,
[3] LTI, UPJV, Amiens, France.

Abstract

This work investigates the study of the experimental weldability in magnetic pulse welding process of a one material assembly (aluminium AA6060T6) and a dissimilar metal couple (aluminium6060T6/copper). The weld quality is defined using a destructive process allowing measuring the weld dimension. A diagram charging voltage-air gap is used to establish the variance of weldability. With the criterion of width of the weld, this representation is able to determine the operational weldability window. The lower boundary is defined by the case of bad weld, i.e. an insufficient bonding, and the upper boundary by defective welds, i.e. a weld susceptible to crack. The weld is able to undergo a plastic deformation prior to failure. A large weld is more potentially ductile. A numerical modelling of a mechanical destructive push out test could be helpful to characterise the weld in a quantitative manner. Finally, the material dissymmetry as considered in this study notably reduces the weldability window because of intermetallic phase at the welded interface. For this case, the weld is found to have a rather brittle behaviour.

Keywords

Cold welding, Condition, Damage.

---

* *This work is based on the results of the project MSIM; the authors would like to thank Le Conseil Régional de Picardie for its financial support.*

1 Introduction

The development of the magnetic pulse welding knows a growing interest since a decade. The process was studied to join multi-material assemblies. Several simple or complex configurations were successfully tested. The process is able to join hybrid structures such as metal/glass or metal/composite and also to weld multi-metal assemblies [1]. As highlighted in several studies, a welded joint is particularly characterized by a wavy shape of the interface. This statement is called into question by Karhaman *et al.*, among others, who noticed that bonding is able to occur at the interface without the wave formation [2]. The presence of the wavy morphology is not necessary to achieve an efficient bonding [2, 3]. The wavy formation may even cause detrimental intermetallic phases [3, 4]. Göbel *et al.* recommended a straight interface rather than a wavy one to avoid harmful intermetallics [3]. This paper investigates the weldability of magnetic pulse welds independently of the wavy or not wavy shape of the interface. A relevant method based on a dimensional criterion of a weld is used to determine the weldabilty. The welding tests are carried out on two cases of assembly: a one material assembly (aluminium AA6060T6) and a dissimilar metal pairs (aluminium6060T6/copper). The effect of material couple on the weldability and on the weld mechanical behaviour is analysed. A numerical approach is developed to characterise the weld in the quantitative manner.

2 Experimental Aspects

2.1 Welding Conditions

The experiment is performed using a Pulsar MPW 25 kJ-9 kV. The machine contains a bank of capacitors for a total capacity of 690 µF which provides an electrical pulse. With the coil used in this study (3 turns coil with a field shaper), the frequency of the pulse is about 10 kHz. The welding principle is well described in [5]. The welding samples consist in tubular assemblies whose geometry and dimensions are given in Figure 1. The flyer is positioned 10 mm inside the field shaper workzone whose length is 15 mm. The results are available for this axial position. Two material couples are studied. The first is an aluminium alloy 6060T6 assembly. The second one is a dissimilar metal assembly (aluminium alloy 6060T6/copper), the substitution of the AA6060T6 stationary part by a Cu one allowing understanding the effect of material couple.

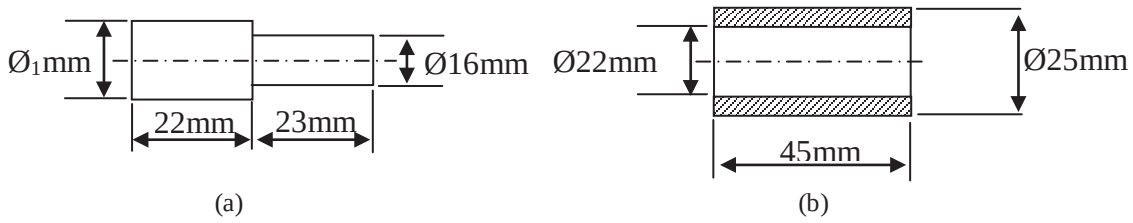

***Figure 1**: Geometry and dimensions of the welding sample - The value of the diameter Ø1 depends on the considered gap*

Several tests with different values for the air gap and the charging voltage are conducted. The axial position of the flyer into field shaper workzone is unchanged. As the

experiments are time consuming, only some of the presented configurations are investigated (Table 1). To summarize the experimental conditions, firstly, the gap was set to 1mm and the charging voltage was varied from 6 kV to 8.5 kV by increment of 0.5 kV. The set parameter (g=1 mm, U=6.5 kV) is found to produce a beginning of weld formation. Secondly, for the charging voltages of 6.5 kV and 7.5 kV, the gap was increased up to 5 mm. Finally, higher voltages and lower gap (0.5 mm) were considered.

	U(kV)						
gap(mm)	5	6	6.5	7	7.5	8	8.5
0.5						A	A
1	C	A C	A C	A C	A C	A C	A
1.5			A C		A C		
2			A C		A C		
2.5			A C		A C		
3			A C		A C		
3.5			A C		A C		
4			A C		A C		
4.5			A C		A		
5			A C		A C		

Table 1: *Set of used parameters for the study (A: AA6060T6 inner part, C: Cu inner part)*

2.2 Weld Characterisation

2.2.1 Dimensional Characterisation

The principle of this characterisation is to measure the length of the joint with a good mechanical bonding. The welded assembly is cut along the revolution axis in several thin samples with a 5 mm thickness. Each sample is then subjected to a manual destructive process: a torque is applied on the flyer in order to break the interface (Figure 2). The fracture surface reveals the zone where there was a good mechanical bond. One observes a residue of the outer tube on the surface of the inner tube (Figure 3). The length of the weld is used to characterise the weld quality. The higher is the length, the better is the weld. In the case of bad weld, the fracture surface does not show any residue.

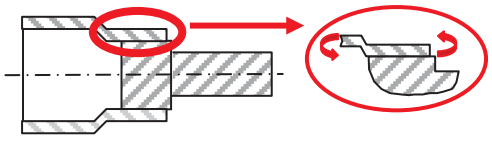

Figure 2*: Illustration of the torque test*

Figure 3*: Illustration of a fracture surface with residue (a) or without residue (b)*

2.2.2 Mechanical Characterisation

A push out test is used to characterise the mechanical features of the weld. The test was performed to specifically load the interface until the rupture of the weld [6]. After welding, the outer tube is machined to keep only the welded part identified by the dimensional characterisation described above. A compression force is applied on the inner tube while the outer tube is contained inside a steel hollow piece (Figure 4). As the welded interface is not parallel to the load direction, it is submitted to combined shear and separation but shear is dominant. After the rupture of the interface, the outer tube is completely pushed out. The analysis of the measured force-displacement curve allows also characterising the mechanical behaviour of the weld.

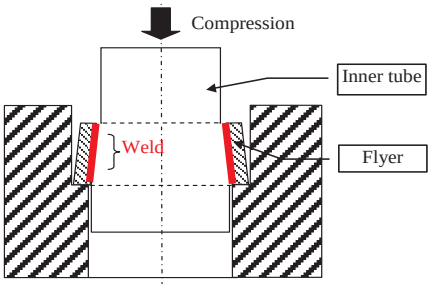

Figure 4: *Illustration of the push-out test [6]*

3 Numerical Aspects

To characterise the weld in a quantitative manner, a finite element model is used to analyse the push out test. Abaqus software is used for this purpose. The meshed finite element model is described in Figure 5. The flyer and the fixed part are discretized using for nodded axisymmetric solid element (CAX4R). The welded interface is modelled using cohesive elements. The other parts involved in the test are considered as rigid body.

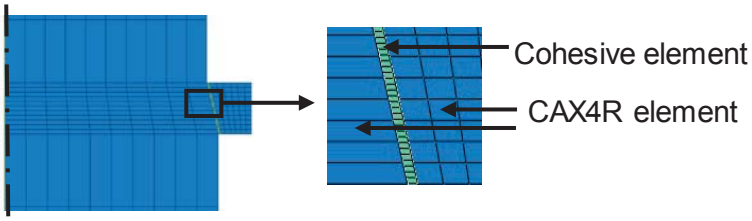

Figure 5: *Illustration of the meshing for the F.E modelling*

For the constitutive modelling, the flyer and the fixed part behaviour are described using simple J2 elastic-plastic model with isotropic work hardening. The interface behaviour is described using a linear traction separation model associated with a progressive damage model. To define the parameters that characterise the interface, the damage initiation and the damage evolution models used in this work are briefly recalled in the following section.

3.1 Damage Initiation

The material degradation process is assumed to begin when the stress or the strain met a certain criteria. In this work, the maximum nominal stress criterion is used:

$$\max\left\{\frac{|t_n|}{t_n^0},\frac{t_s}{t_s^0},\frac{t_t}{t_t^0}\right\}=1 \tag{1}$$

t_n is nominal stress in the direction normal to the interface, and t_n^o peak value. t_s and t_t are the nominal stress in the first and second shear direction. Likewise, t_s^o and t_t^o are their respective peak value. The overall objective of this model is to predict the damage initiation of reliable welded joint. For this reason, the discontinuities inherent to the welding process are not taken into account as initial damage.

3.2 Damage Evolution

A simple linear damage evolution is considered to describe the progressive damage at the interface. A criterion of energy dissipated due to failure is used to the definition of the damage evolution. The scalar damage variable, namely D, is a function of the effective displacement at the interface:

$$D=\frac{\delta_m^f\left(\delta_m^{\max}-\delta_m^0\right)}{\delta_m^{\max}\left(\delta_m^f-\delta_m^0\right)} \tag{2}$$

$\delta_m^{\max}$ is the maximum value of the effect displacement reached during the loading history, and δ_m^0 the effective displacement at damage initiation. δ_m^f is the effective displacement at damage initiation at complete failure which is defined as a function of the fracture energy as follows:

$$\delta_m^f=\frac{2G^c}{T_{eff}^0} \tag{3}$$

T_{eff}^0 is the effective traction at damage initiation and G^c the fracture energy that is the input damage parameter to describe the damage evolution.

After the damage initiation, the stress components of the traction-separation model are degraded by the damage evolution as follows:

$$t_n=\begin{cases}(1-D)\overline{t}_n, \overline{t}_n\geq 0\\ \overline{t}_n,\end{cases} \tag{4}$$

$$t_s=(1-D)\overline{t}_s, \tag{5}$$

$$t_t = (1-D)\bar{t}_t \quad (6)$$

where the notation $\bar{t}$ means stress components calculated by the traction-separation behaviour for the current strains without damage. The set of parameters describing the interface behaviour i.e. the nominal peak stresses and the fracture energy are adjusted to reproduce the experimental evolution of the measured push-out force versus displacement.

4 Results and Discussion

4.1 Weld Characteristic

The weldability study of the aluminium AA6060T6 assembly allows providing further insights into the features a weld. The dimensional characterisation highlights four weld kinds that are obtained by increasing the air gap value rather than the charging voltage. There is a bad weld, a thin ring-shaped weld, a large and potentially ductile weld and lastly, a large joint with discontinuous voids. The bad weld is a case of an insufficient bonding. The interfacial bond breaks while the welded assembly is cut in the revolution axis because of the relaxation of the residual stress in the outer part due to the shrinking occurring within the compression of the outer tube. The fracture surface looks like an adhesive fracture (Figure 6a). The destructive torque test reveals as a beginning of a good bonding, a thin weld with a ring shape (Figure 6b). With the gap increase, the weld becomes larger and the fracture surface after the torque test shows an area with a circular path (Figure 6c). Indeed, the interfacial residue reveals a rotational deformation under the action of the torque load. Then, the weld is potentially ductile. Above a critical air gap value, it has been observed that the welded interface contains discontinuous voids (Figure 7). This damage is attributable to a strong interfacial shearing due to high impact velocity occurring at high gap. This defect decreases the effective bonding surface and creates crack initiations that could be detrimental to the integrity of the joint.

(a) (b) (c)

***Figure 6**: Illustration of a bad weld (a), a thin ring-shaped weld (b) and a large weld (c)*

***Figure 7**: Illustration of a welded interface with discontinuous voids*

The typical mechanical behaviour of the weld previously identified is compared in Figure 8. The push out test has evidenced an elastic-plastic behaviour of both thin and large weld. This result proves that the interface is able to undergo plastic deformation prior to failure. The large weld is more potentially ductile. Moreover, a good weld reveals a ductile damage behaviour. If the joint contains discontinuous voids, the weld still has a

plastic behaviour but the rupture occurs brutally. The measured force quickly collapses during the failure.

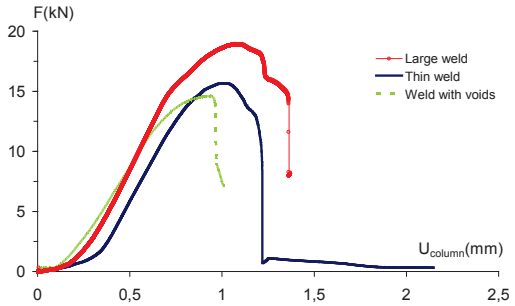

***Figure 8**: Illustration of the typical behaviour of the identified weld –The non linear response at the beginning of the measure is attributable to the contact accommodation*

The numerical model of the push-out test predicts the force/displacement response prior to failure (Figure 9). The simulation does not account for the initial curve due to sliding at the contact surfaces. The numerical result is also able to reproduce the failure response of the weld as shows the Figure 9. The numerical model is currently developed to accurately predict the weld mechanical behaviour. This strategy may be helpful to found quantitative correlations between the joining process parameters, the structure of the interface and its mechanical behaviour.

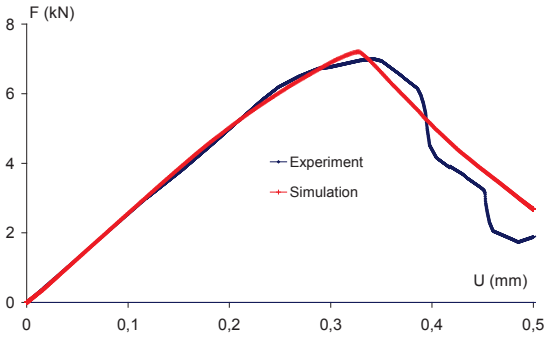

***Figure 9**: Illustration of a comparison between the numerical and the experimental result*

4.2 Weldability Window

In impact welding, as the precise mechanism of the weld formation is still misunderstood, the elaboration of weldability window remains problematic. Deribas *et al.* [7] suggested a weld lobe depending on the collision angle and the impact velocity. The authors used as weld criterion the formation of the interfacial wavy shape that is found to be predicted by this couple of parameters. Zhang *et al.* [8] brought an experimental approach to build such a weldability window by measuring the welding velocity and deducing the collision angle. The operational window is obtained for a range of low value of the collision angle. Uhlmann and Ziefle [9] claimed that weld formation depends on several parameters and could occur even at high collision angle. Situations of low collision angle without weld formation have also been observed. Dhanesh et al [10] used numerical simulation to build weldability windows for sheet metal joining taking into account several process parameters. In our study, a practical way to define the weldability is suggested. The weld

variance is presented in a chart defined by the main monitorable process parameters, i.e. the charging voltage (U) and the air gap (g). The bad welds are generally obtained at low gap because of insufficient impact velocity and probably low collision angle. The set of (U,g) values resulting in bad welds determines the lower boundary of the weldability window. Given that a sufficiently high gap damages the welded interface by creation of discontinuous voids, this detrimental condition defines the upper boundary. According to this representation, the range of good weld is wide for the case of similar aluminium AA6060T6 assembly (Figure 10). As presented in the next section, the substitution of the aluminium inner tube by a copper one strongly influences this welding range.

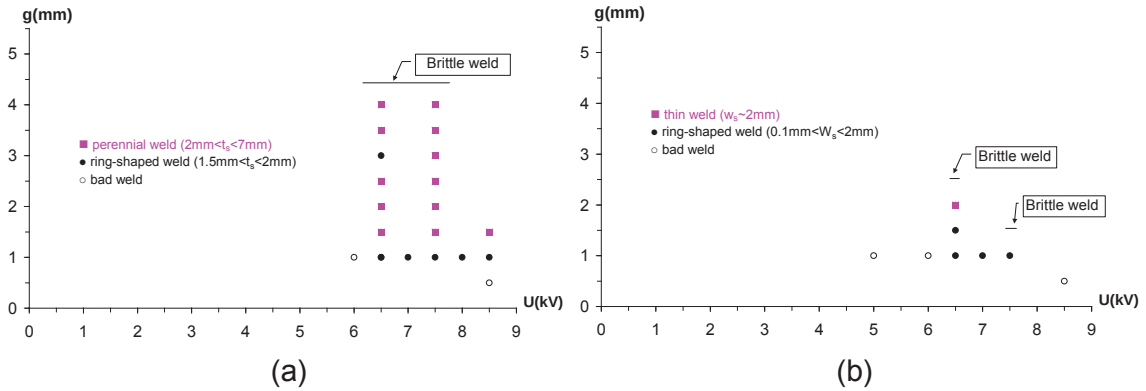

***Figure 10**: Operational welding range - (a): case of AA6060T6 pair assembly, (b) case of AA6060T6/Cu assembly*

As the impact velocity is the parameter involving all interfacial mechanisms, such a weldability window enables to provide a welding range using velocity isovalues. Hence, this approach is able to highlight different effects of process parameters and then to provide further insights into ways of optimizing the process by velocity measurements.

4.3 Effect of Dissimilar Material Pairs

The combination of the aluminium AA6060T6 with copper leads to a formation of an intermetallic phase at the interface during the welding. Zhang *et al.* [11] state that the mechanism of diffusion could occur at the interface but in a very short distance (some nm) whereas the intermallic thickness is in the order of µm. Several studies claim that this phase is a consequence of local fusion at the interface followed by a rapid solidification with a high cooling rate. Faes *et al.* [4] found an evidence of fusion at interface MPW weld joint using SEM analysis. Elsen *et al.* [12] performed a numerical simulation of the MPW of an aluminium AA6000 tube that includes the heating effect due to high deformation at interface. The results predict an impact velocity of around 300 m/s and an interfacial temperature level of 1400 °C, largely exceeding thereby the melting temperature of the aluminium. Göbel *et al.* [3] mentioned that the Al/Cu dissimilar interface produces an Al rich intermetallic phase obtained under strong non equilibrium conditions. The intermetallic phase could appear as a continuous layer with a thin or wide thickness, or as a pocket developed at wave crests in case of wavy interface [1, 3]. TEM analysis of a Al/Cu weld revealed that the intermetallic consists in amorphous phase [13]. It is the presence of this intermetallic phase that significantly reduces the operational welding

range (Figure 10). The dimensional characterisation showed that the widest length of an Al/Cu weld is tree times lesser than these of the Al/Al case. For the Al/Cu welds obtained at extreme gaps, the destructive torque test does not reveal any residue as seen in the case of Al/Al weld (Figure 11). Göbel *et al.* [3] investigated the intermetallic structure of an Al/Cu weld and correlate the weld integrity to the intermetallic thickness. Thick intermetallics contain detrimental defects such as voids, pores and cracks. The intermetallic is found to have a critical thickness minimizing those defects. Decreasing the impact energy is claimed to reduce the intermetallic thickness [3, 4]. This explains the lowering of the upper boundary of the weldability window when the aluminium inner tube is substituted by a copper one (Figure 10).


(a) (b)

***Figure 11**: Typical fracture surface of Al/Cu weld - (a): relatively good weld, (b): weld with intermetallic phase*

The intermetallic influences also the mechanical behaviour of the weld. The presence of amorphous intermetallic phase makes the weld brittle. Typical mechanical behaviours of Al/Cu and Al/Al welded joints are given in Figure 12. For the Al/Cu joint, the observed post fracture residual force is due to the deep penetration of the aluminum flyer into the copper part.

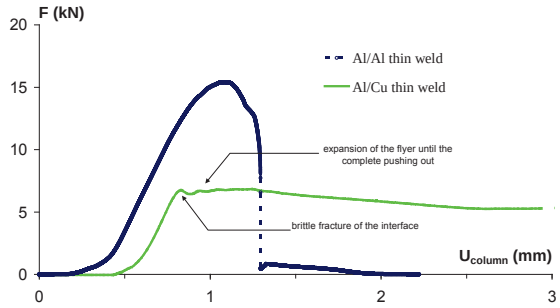

***Figure 12**: Typical mechanical behaviour of a thin Al/Al weld and Al/Cu weld*

5 Conclusions

The weldability of aluminium AA6060T6 tubular assembly is studied in this paper. The weldability is characterised by a dimensional criterion given by a destructive torsion test. The test highligths four weld cases: a bad weld, a thin ring-shaped weld, a large and potentially ductile weld and lastly, a large weld but with discontinuous voids. The bad weld is a case of an insufficient bonding. The destructive push out test revealed an elastic-plastic behaviour of both thin and large weld. The large weld is more potentially ductile and besides, evidenced a rather ductile damage behaviour. In case of weld with discontinuous voids the rupture occurs brutally. The numerical model of the push out test is able to reproduce the interface behaviour. The set of (charging voltage, air gap) values resulting in defective welds are able to represent the lower and upper boundary of the weldability window. The substitution of the aluminium inner tube by a copper one leads to

an intermetallic phase which strongly lowers the upper boundary. The intermetallic influences also the mechanical behaviour of the weld. The weld becomes more brittle.

References

[1] *Kashani, M.; Aizawa, T.; Okagawa, K.:* Welding and Forming of Sheet Metals Using Magnetic Pulse Technology. Proceedings of the 4th International Conference on High Speed Forming, Columbus-Ohio, USA, 2010.

[2] *Kahraman, N.; Gülenç, B.:* Microstructural and mechanical poreprties of Cu-Ti plates bonded through explosive welding process. J. Mat. Proc Technol., 169, p. 67-71, 2005.

[3] *Göbel, G.; Kaspar, J.; Herrmannsdörfer, T.; Brenner, B., Beyer; E.:* Insights into intermetallic phases on pulse welded. Proceedings of the 4th International Conference on High Speed Forming, Columbus-Ohio, USA, 2010, p. 127-136.

[4] *Faes, K.; Baaten, T.; De Waele, W.; Debroux, N.:* Joining of Copper to Brass Using Magnetic Pulse Welding. Proceedings of the 4th International Conference on High Speed Forming, Columbus-Ohio, USA, 2010, p. 84-96.

[5] *Shribman, V.:* Magnetic Pulse welding for dissimilar and similar materials. Proceedings of the 3rd International Conference on High Speed Forming, Dortmund, 2008, p. 13-22.

[6] *Raoelison, R.N.; Buiron, N.; Habak, M.; Haye, D.; Rachik, M.:* Elastoplastic and Damage Behaviour of Magnetic Pulse Weld Interfaces. Proceedings of the 10th International Conference on Technology of Plasticity, Aachen, Germany, 2011, p. 1160-1163.

[7] *Deribas, A.A.; Simonov, V.A.; Zakcharenko, I.D.*: Investigation of the explosive parameters for arbitrary combinations of metals and alloys. Proceedings of the 5th International Conference on High Energy Rate Fabrication, Denver-Colorado, USA, 1975, p. 1-24.

[8] *Zhang, Y.; Babu, S.; Daehn, G.S.:* Impact Welding in a Variety of Geometric Configurations. Proceedings of the 4th International Conference on High Speed Forming, Columbus-Ohio, USA, 2010, p. 97-107.

[9] *Uhlmann, E.; Ziefle, A.:* Modeling Pulse Magnetic Welding Processes – An Empirical Approach. Proceedings of the 4th International Conference on High Speed Forming, Columbus-Ohio, USA, 2010, p. 108-116.

[10] *Dhanesh; P.C.; Kore; S.D.; Date; P.P.:* A Numerical Criterion for The Formation of A Solid State Welded Joint in Sheets by Electromagnetic Forming/Joining. Proceedings of the 10th International Conference on Technology of Plasticity, Aachen, Germany, 2011, p. 1154-1159.

[11] *Zhang, Y.; Babu, S.; Zhang, P., Kenik, E.A., Daehn, G.:* Microstructure characterisation of magnetic pulse welded AA6061-T6 by electron backscattered diffraction. Sci. Technol. Weld. Joining, 2008, p. 467-471.

[12] *Elsen, A.; Ludwig, M.; Schaefer, R.; Groche, P.:* Fundamentals of EMPT-Welding. Proceedings of the 4th International Conference on High Speed Forming, Columbus-Ohio, USA, 2010, p. 117-126.

[13] *Watanabe, M.; Kumai, Shinji.:* Welding interface in magnetic pulse welded joints Materials Science Forum, 2010, p. 654-656.